# A New Method for Metal Artifact Reduction in CT

Thomas Koehler,[a] Bernhard Brendel,[a] and Kevin M. Brown[b]

*Abstract*—**In this work, we present a new method for metal artifact reduction in computed tomography (CT), which is based on a sinogram interpolation technique. The method further comprises an adaptive application of the correction image which is specifically designed to avoid that the correction introduces new artifacts. The method is evaluated using clinical data.**

## I. Introduction

The presence of metal within the field of view of a CT scanner can create severe artifacts in the reconstructed images. There are several different physical origins of these artifacts and the appearance of the artifacts can be very different, too [1]: Metal causes beam-hardening, resulting in dark and bright shading artifacts, in particular dark shading between metal objects, e. g., between two hip implants. Metal has a large linear attenuation coefficient leading to photon starvation in the shadow of the metal object, which can result in severe noise streaks. The large contrast of metal objects makes the CT imaging chain more sensitive to patient motion, which can lead to streak-shaped or arc-shaped artifacts for axial or helical acquisitions, respectively [2]. Furthermore, the contribution of scattered photons to the detected signal in the metal shadow is typically large, resulting also in dark and bright shading artifacts.

There are a lot of methods for metal artifact reduction (MAR): Noise streaks due to photon starvation can be suppressed by adaptive filtering [1,3]. Beam hardening can be addressed by beam hardening correction algorithms [1, 4].

Another common and completely different approach for MAR is to replace data in the metal shadow in the sinogram by something more meaningful. The shadow is typically identified by segmentation in image domain followed by a forward projection. The replacement can be done by interpolation [2,3,5–9], or by a re-projection of a segmented image [10–13].

More recently, several iterative methods for MAR have been proposed [14–16]. Although statistical iterative methods are in general less sensitive to metal artifacts since the statistical weight for data in the metal shadow are small due to their bad statistics, they cannot reduce beam-hardening artifacts unless they contain a metal segmentation step.

MAR has been an area of active research for more than 30 years now, indicating that it is in fact a very tough problem. From our point of view, the major problem with MAR algorithms is robustness: Since the effects which lead to the artifacts and the appearance of the artifacts can be quite different, it is hard to set up an algorithm that handles every case well. Furthermore, many of the advanced methods contain a segmentation step in the processing chain. However, we observed that the artifacts in the original images can be so severe that a reliable segmentation is not possible, often leading not only to an imperfect correction of the metal artifacts but rather to the introduction of new artifacts. While an imperfect or incomplete correction of the metal artifacts may be acceptable in a clinical use case, the introduction of new artifacts is not.

This work contains two new contributions to the art of MAR: The first one is a further improvement of the algorithm proposed by Timmer [11]. The second is a general idea related to artifact correction methods in CT that aims specifically at preventing the introduction of new artifacts.

## II. Method

First, we briefly review the method described by Timmer [11] and discuss its shortcomings.[1] The basic idea of the algorithm is to replace the data in the metal shadow by something more meaningful than the linear interpolation used by Kalender et al. [6]. In detail, the method comprises the following steps:

1. generation of an initial image using filtered back-projection,
2. classification of the pixels in the initial image into metal, bone, soft tissue, and air by thresholding,
3. generation of a metal only sinogram by forward projecting the pixels classified as metal,
4. generation of a synthetic image by replacing the pixels belonging to the soft tissue class by their mean pixel value (keeping bone and metal pixels unchanged),
5. generation of a synthetic sinogram by forward projecting the synthetic image,
6. replacing the line integrals in the metal shadow by the synthetic sinogram values (including a linear baseline shift to ensure that the replacement fits continuously to the data), and
7. generation of the corrected image by filtered back-projection of the new sinogram.

The use of the forward projected synthetic image to fill the metal shadow gives a realistic estimate of the missing data. The classification step is intended to avoid that streak or shading artifacts propagate through the processing chain into the corrected image.

The first shortcoming of this algorithm is that the classification procedure sometimes fails in the presence of severe beam-hardening artifacts. This issue was addressed by Schmitt et al. [17] by performing the classification step on an image that is already corrected by Kalenders algorithm.

[a] Philips Technologie GmbH, Innovative Technologies, Research Laboratories, Hamburg, Germany
[b] Philips Healthcare, Cleveland, OH, USA

[1] We always use additionally an adaptive filtering step in order to suppress high frequency streak patterns.

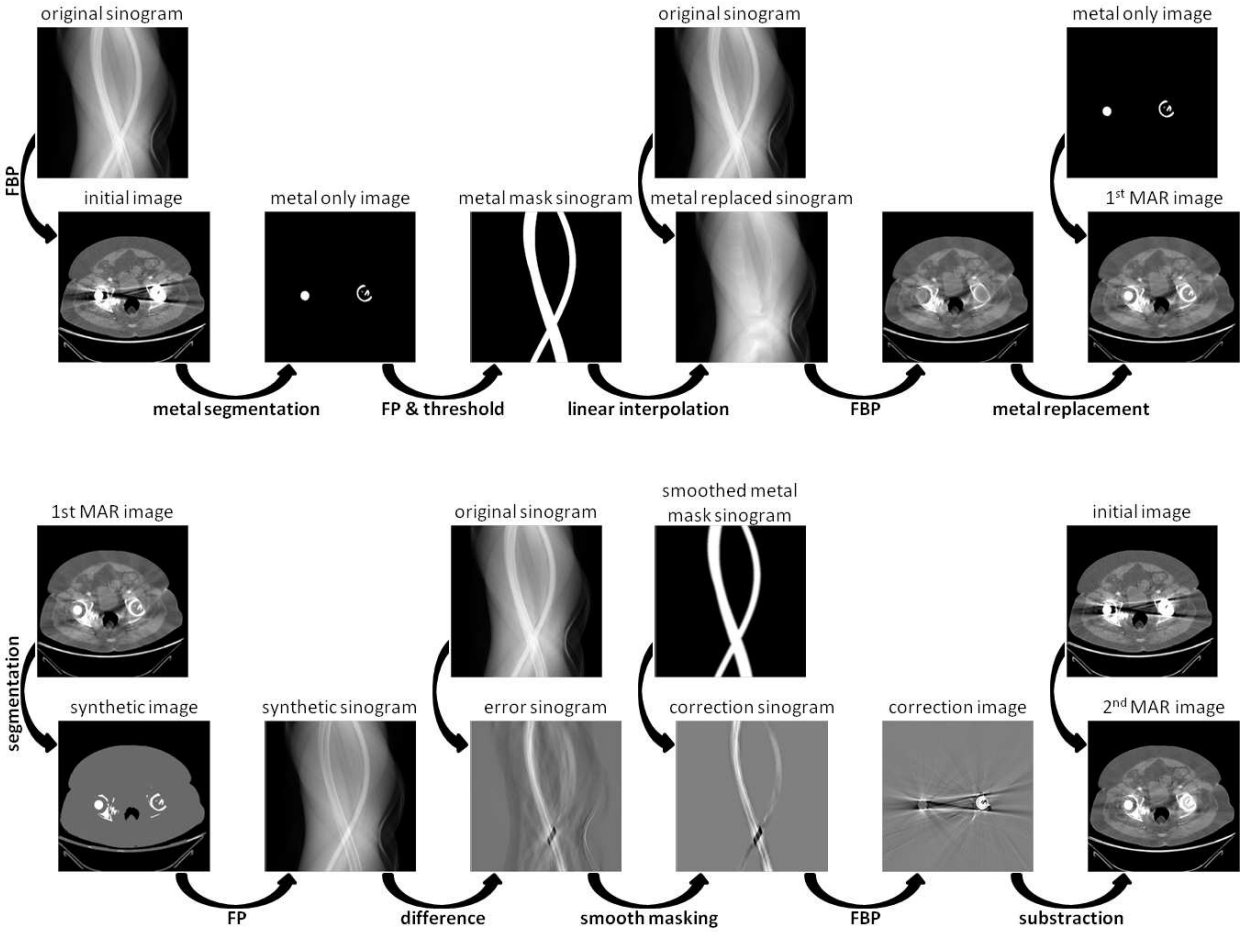


Fig. 1. Flow chart of the proposed MAR algorithm. The lower processing may be executed multiple times.

Another shortcoming is that the linear baseline correction in the metal shadow replacement step ensures a continuous fit of the synthetic sinogram data but not a smooth fit. Consequently, there is still a fair likelihood that streak artifacts are generated. This problem is addressed in the new algorithm by the introduction of a smooth fading of the synthetic sinogram data into the metal shadow. Another minor change is that we do not explicitely interpolate across the shadow, but rather calculate a correction sinogram. These changes lead to the following processing scheme, which is also illustrated in Fig. 1:

1. Initial MAR:

(a) generation of an *initial image* by an FBP reconstruction,

(b) generation of a *metal only image* by thresholding,

(c) generation of a *metal mask sinogram* by forward projection of the metal only image followed setting all non-zero values to one,

(d) generation of a *metal replaced sinogram* by linear interpolation across the metal shadow in the original sinogram, and

(e) generation of a $1^{st}$ *MAR image* by filtered backprojection of the metal replaced sinogram.

2. $2^{\text{nd}}$ pass MAR:

(a) generation of a *synthetic image* as in the original method by Timmer from the $1^{\text{st}}$ MAR image,

(b) generation of a *synthetic sinogram* by forward projection,

(c) generation of an *error sinogram* as the difference of the synthetic sinogram and the original sinogram,

(d) generation of a *correction sinogram* by multiplying the error sinogram with a smoothed version of the metal mask sinogram,

(e) generation of a *correction image* by filtered backprojection of the correction sinogram, and

(f) generation of the $2^{nd}$ *MAR image* by subtracting the correction image from the original image.

We note that the artifact reduction can be further improved by running a $3^{\text{rd}}$ pass with the $2^{\text{nd}}$ MAR image as input. The original sinogram can be either the acquired sinogram or a synthesized one re-projected from the original image. Using the synthesized sinogram results typically in only slightly worse results, but the processing is much faster since 2D processing can be used. For the images in this paper, the second method is used.

Even though the smoothed metal mask sinogram is used to generate the correction sinogram, we still observe occasionally some newly introduced streak artifacts. Furthermore, inaccuracies in the segmentation and classification can lead to some artificial dark or bright shading in the final image. These remaining problems can be addressed by the following idea of *adaptive application of the correc-*

*tion image*: The starting point for the idea is the fact that the correction image is supposed to show just the artifacts which are present in the initial image. In other words, the intention of the last processing step, namely the image subtraction, is to remove structured features from the initial image. This observation leads to the idea of performing the last step locally, if and only if, the amount of structure in the obtained image is reduced. One straight forward realization of this idea is to locally weight the correction image with a weighting factor. If this weighting factor is allowed to take values smaller or larger than one, the method can also correct locally an over- or under-estimation of the strength of the metal artifacts.

We formulate this method using the following definitions: The $N \times N$ initial image is denoted as $I$ with individual pixels $I_{ij}$. The correction image and its pixels are denoted as $C$ and $C_{ij}$, respectively. For a given index pair $(k, l)$ we denote a sub-image of $I$ containing the neighborhood of the image pixel $I_{kl}$ as $\mathcal{N}_{kl}(I)$. We further assume to have a structure measure $S$ that gives for any image a quantitative measure for the amount of structure in the image. Details about the neighborhood and the structure measure will be given later. Using these definitions we can formulate the calculation of a weighting image $W$ by

$$W_{kl} = \arg\min_{w} S\left(\mathcal{N}_{kl}(I) - w\mathcal{N}_{kl}(C)\right) \tag{1}$$

and the final image metal artifact corrected image $F$ is defined by

$$F_{kl} = I_{kl} - W_{kl}C_{kl}\,. \tag{2}$$

For the evaluation of this approach we need to pick a structure measure and a certain neighborhood. Several options are at hand for the structure measure like the variance of the image values or their total variation. Here, we use the entropy of the normalized histogram of the image as structural measure. The default bin size for the histogram is 10 HU. The neighborhood $\mathcal{N}_{kl}(I)$ of the pixel $I_{kl}$ is by default a $11 \times 11$ patch centered around the pixel $I_{kl}$. In a few special cases, we observed that the shading artifacts in the correction image are so large and smooth that the default neighborhood of $11 \times 11$ is too small in order to be able to calculate appropriate weighting factors using Eq. (1) since the structure measure is insensitive to just changing all pixel values by the same correction value. In this case, the neighborhood can be adaptively enlarged in order to ensure that $\mathcal{N}_{kl}(C)$ has sufficient structure.

## III. Results

The proposed method was tested on a couple of clinical cases. Fig. 2 shows the performance of the new algorithm applied to a few example cases. For illustration purpose, we show in addition to the initial, uncorrected image and the final, fully corrected image also the result of the algorithm without the last step of adaptive application of the correction image, i. e. the images obtained using a weighting image $W$ that is a constant unity image. Please note that we selected only examples, where the algorithm without adaptive application of the correction image does in fact introduce some new artifacts, which happens only in rare cases. However, we selected these examples to show the importance and effectiveness of the additional step of adaptive application of the correction image.

The top row of Fig. 2 shows a case with bilateral hip replacement. The dominant artifact in the initial image is the dark broad streak between the two hips. This dominant artifact is well reduced using the plain MAR algorithm. However, it also introduces a few minor streak artifacts (indicated by arrows). The use of the adaptive application of the correction image avoids the introduction of these artifacts while still removing the dominant ones.

The middle row of Fig. 2 shows a case with a ventricular assist device. The dominant artifacts in the initial image are streaks emanating from the electrode and the battery. Again, the plain MAR algorithm reduces the dominant artifacts substantially. However, it also introduces a lot of low frequency artifacts, in this case most likely because the contrast agent in the ventricle and the aorta is classified as soft-tissue. As in the first case, the adaptive application of the correction image avoids the introduction of these artifacts while still removing the dominant one.

The bottom row of Fig. 2 shows another slice of the same case as in the middle row. The dominant artifact in the initial image are two streaks connecting the metal objects. These streaks are reduced considerably by the plain MAR algorithm (although not completely, see arrow), but some shading artifacts are introduced (indicated by a circle in the middle column). Again, the adaptive application of the correction image preserves the suppression of the metal artifacts while at same time it does not introduce new artifacts.

## IV. Discussion

MAR has been a field of active research for more than 30 years now. This long history and the fact that it was only recently introduced commercially on a clinical scanner indicates that MAR is a very difficult problem. We presented in this work two new contributions to the art of MAR. The first one is a basic MAR algorithm that works well already in most cases. The second one is the idea of adaptive application of the correction image, which is specifically designed to avoid the introduction of new artifacts in the image after application of MAR. We would like to stress that the second idea can be applied to any MAR algorithm as long as this algorithm can be formulated as a subtraction of an correction image from an initial image, which is in most cases possible, at least in FBP based methods.

The idea of adaptive application of the correction image requires a choice for a structure measure and for a neighborhood. So far we obtained decent results using the entropy as a structure measure and a $11 \times 11$ neighborhood that can be further enlarged if the sub-image of the correction image does not contain sufficient structure. However, the optimization of this structure function is rather slow since a lot of evaluations of the logarithm are required. Thus, further investigations in this area comparing effectiveness

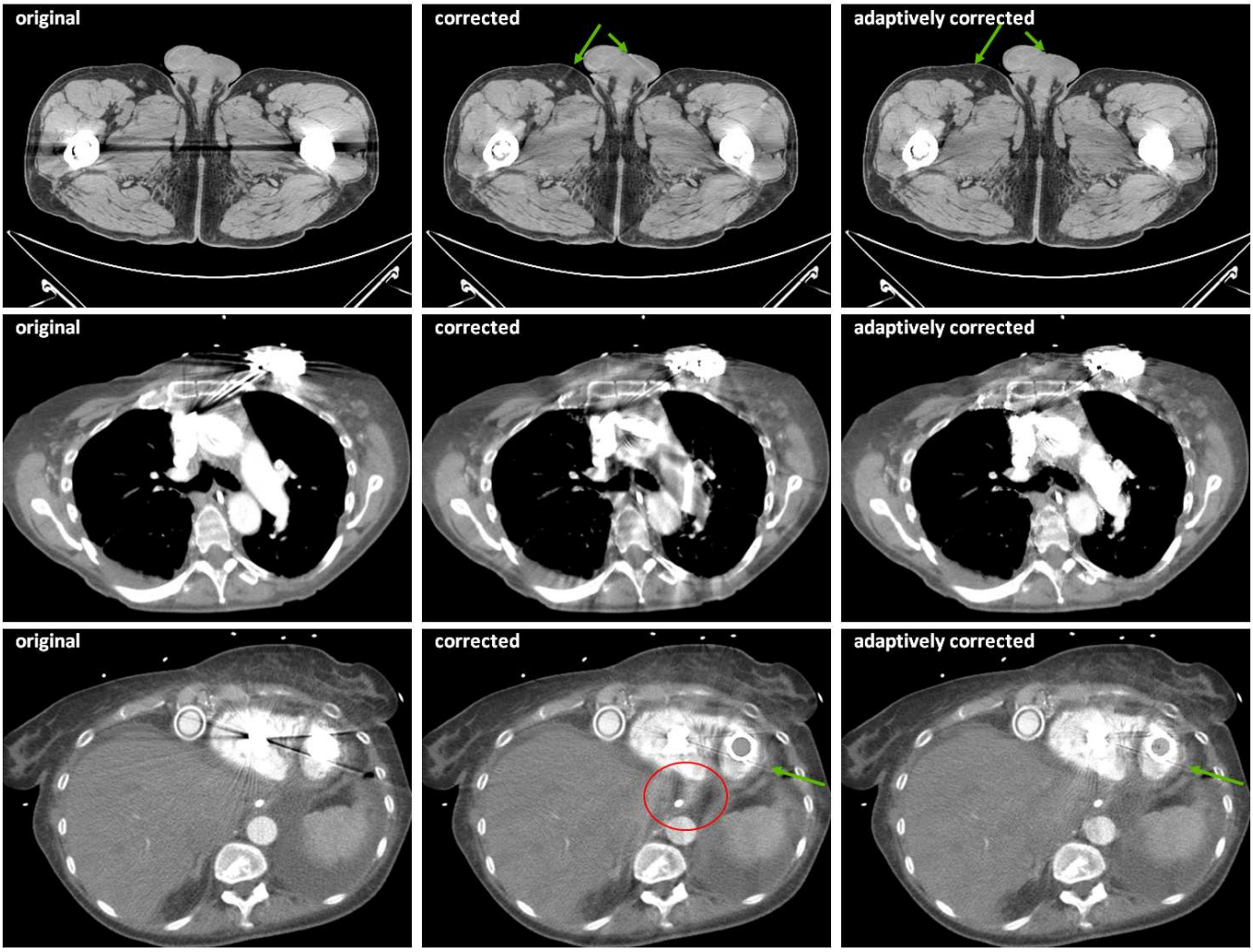


Fig. 2. Results of the proposed method. Left column: initial images with metal artifacts. Middle column: Result of the proposed method without adaptive application of the correction image. Right column: Result of the proposed method with adaptive application of the correction image. Level and window are 0 HU and 500 HU, respectively.

and speed of different structure measures are desirable.

## References


[1] J. Hsieh, *Computed Tomography - Principles, Design, Artifacts, and Recent Advances*, SPIE, Bellingham, Washington, 2003.

[2] G. H. Glover and N. J. Pelc, "An algorithm for the reduction of metal clip artifacts in CT reconstructions," *Med. Phys.*, vol. 8, no. 6, 799–807, 1981.

[3] O. Watzke and W. A. Kalender, "A pragmatic approach to metal artifact reduction in CT: merging of metal artifact reduced images," *European Radiology*, vol. 14, no. 5, 849–856, 2004.

[4] B. De Man, J. Nuyts, P. Dupont, G. Marchal, and P. Suetens, "An iterative maximum-likelihood polychromatic algorithm for CT," *IEEE Trans. Med. Imag.*, vol. 20, no. 10, 999–1008, 2001.

[5] R. M. Lewitt, "Processing of incomplete measurement data in computed tomography," *Med. Phys.*, vol. 6, no. 5, 412–417, 1979.

[6] W. A. Kalender, R. Hebel, and J. Ebersberger, "Reduction of CT artifacts caused by metal implants," *Radiology*, vol. 164, 576–577, 1987.

[7] A. H. Mahnken, R. Raupach, J. E. Wildberger, B. Jung, N. Heussen, T. G. Flohr, R. W. Günther, and S. Schaller, "A new algorithm for metal artifact reduction in computed tomography: in vitro and in vivo evaluation after total hip replacement," *Investigative Radiology*, vol. 38, no. 12, 769–775, 2003.

[8] J. Wei, L. Chen, G. A. Sandison, Y. Liang, and L. X. Xu, "X-ray CT high-density artefact suppression in the presence of bones," *Phys. Med. Biol.*, vol. 49, no. 24, 5407–5418, 2004.

[9] E. Meyer, R. Raupach, M. Lell, B. Schmidt, and M. Kachelriess, "Normalized metal artifact reduction (NMAR) in computed tomography.," *Med. Phys.*, vol. 37, no. 10, 5482–5493, 2010.

[10] H. K. Tuy, "A post-processing algorithm to reduce metallic clip artifacts in CT images," *European Radiology*, vol. 3, 129–143, 1993.

[11] J. Timmer, "Metal artifact correction in computed tomography," 2003, US 7340027 B2.

[12] M. Bal and L. Spies, "Metal artifact reduction in CT using tissue-class modeling and adaptive prefiltering," *Med. Phys.*, vol. 33, no. 8, 2852–2859, 2006.

[13] D. Prell, Y. Kyriakou, M. Beister, and W. A. Kalender, "A novel forward projection-based metal artifact reduction method for flat-detector computed tomography," *Phys. Med. Biol.*, vol. 54, no. 21, 6575–6591, 2009.

[14] T. Buzug and M. Oehler, "Statistical image reconstruction for inconsistent CT projection data," *Methods Inf. Med.*, vol. 46, no. 3, 261–269, 2007.

[15] C. Lemmens, D. Faul, and J. Nuyts, "Suppression of metal artifacts in CT using a reconstruction procedure that combines MAP and projection completion.," *IEEE Trans. Med. Imag.*, vol. 28, no. 2, 250–260, 2009.

[16] H. Xui, L. Zhang, Y. Xing, and Z. Chen, "An iterative reconstruction technique for metal artifact reduction," in *Proceedings of the Fully3D/HPIR*, 2011, 199–202.

[17] H. Schmitt, J. Timmer, and T. Köhler, "A three-pass method for metal artifact reduction in computed tomography," in *Med. Phys.*, 2007, vol. 34, 2571.